

Direct experimental observation of the Hall angle in the low-temperature breakdown regime of n -GaAs

V. Novák

Institute of Electrical Engineering AS CR, Dolejškova 5, 182 02 Praha, Czech Republic

J. Hirschinger, F.-J. Niedernostheide,* and W. Prettl

Institut für Experimentelle und Angewandte Physik, Universität Regensburg, 930 40 Regensburg, Germany

M. Cukr and J. Oswald

Institute of Physics AS CR, Cukrovarnická 10, 162 53 Praha, Czech Republic

(Received 8 July 1998)

Using the technique of photoluminescence imaging during electrical transport in crossed electric and magnetic fields, the rotation of the current flow direction has been observed. The rotation angle is identically the Hall angle. As a model system, a thin n -type GaAs layer in the regime of low-temperature impurity breakdown has been used, generating filamentary current patterns. The measurement of the Hall angle allows one to determine the mobility inside current filaments. [S0163-1829(98)05043-7]

The Hall effect is the most important probe of transport properties in semiconductors. In standard measurements of the Hall effect the material properties of interest are calculated from voltage drops obtained by potential probes. Interpretation of such measurements must take into account the particular geometry of the investigated sample. So, for example, across a bar-shaped sample the transversal electric field \mathcal{E}_H , the Hall field, is measured. Through the ratio of the Hall field to the longitudinal driving electric field \mathcal{E}_l the value of Hall angle can be obtained, $\theta_H = \arctan(\mathcal{E}_H/\mathcal{E}_l)$, which is directly related to the charge-carrier mobility. The above formula is often understood as a definition of the Hall angle; its validity is, however, strictly bound to a bar shaped sample. Generally, the Hall angle is defined as the angle between the current density vector and the local electric-field vector in the presence of a perpendicular magnetic field. Since it is independent of a particular sample geometry and even of material inhomogeneities, the Hall angle represents a fundamental intrinsic physical quantity in galvanomagnetic transport. In spite of this fact, to our knowledge it has not been directly measured so far.

Here we report on an experiment where an image of the current flow has been obtained and the Hall angle has been measured by a protractor. The measurements have been carried out on epitaxial layers of n -type GaAs at liquid-helium temperature, making use of the fact that the current flow in samples of this material is inherently inhomogeneous due to the self-organized formation of current filaments. The current filamentation occurs in slightly doped semiconductors at low temperatures if the material is driven by an external voltage bias into electric breakdown due to impact ionization of shallow impurities.^{1,2} The filamentary current pattern, and thus the direction of current flow, can be visualized by photographing the sample photoluminescence.^{3,4} An example of such a visualization is shown in Fig. 1(a). The dark vertical stripe corresponds to a stable self-organized current filament nucleated between two parallel Ohmic contacts which appear as dark horizontal stripes at the top and bottom of the figure.

If a magnetic field is applied perpendicular to the epitaxial layer, the current flow direction deflects from the orientation of the electric field imposed by the contacts, as seen in Figs. 1(b)–1(e). The filament tilting angle rises monotonically with increasing strength of the magnetic field. It can straightforwardly be identified with the Hall angle.

The transport of electrons in a semiconductor layer in crossed electric and magnetic fields can be described in terms of the generalized Ohm's law, where the conductivity has the form of a second-rank tensor,^{5–7}

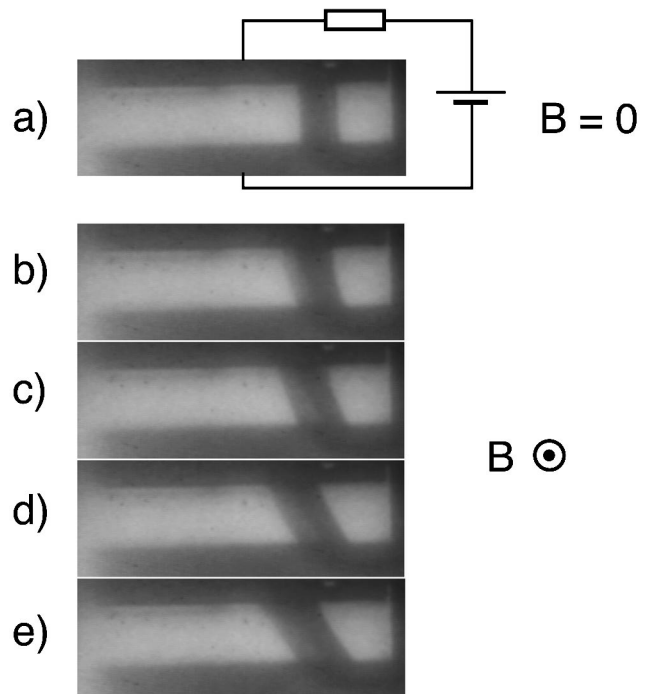


FIG. 1. Visualization of the filamentary current flow at a constant sample current $I = 1$ mA and (a) $B_z = 0$, (b) $B_z = 64$ mT, (c) $B_z = 126$ mT, (d) $B_z = 188$ mT, and (e) $B_z = 251$ mT.

$$\mathbf{j} = b_M \sigma_0 \begin{pmatrix} 1 & -r_H \mu B_z \\ r_H \mu B_z & 1 \end{pmatrix} \mathcal{E}. \quad (1)$$

Here $\mathbf{j} = (j_x, j_y)$ is the current density, $\mathcal{E} = (\mathcal{E}_x, \mathcal{E}_y)$ is the electric field, and B_z is the normal magnetic field. $\sigma_0 = e \mu n$ and $\mu = e \langle \tau \rangle / m^*$ are the conductivity and the electron mobility in case of zero magnetic field, respectively. $\langle \tau \rangle$ is the electron scattering time averaged over the electron distribution function, and m^* , n , and e denote the effective mass of electrons, their density, and the elementary charge, respectively. The dimensionless coefficients b_M and r_H depend, through τ , on the actual scattering mechanisms and are generally B_z dependent:

$$b_M = \left\langle \frac{\tau}{1 + (\omega_c \tau)^2} \right\rangle \langle \tau \rangle^{-1}, \quad (2a)$$

$$r_H = \left\langle \frac{\tau^2}{1 + (\omega_c \tau)^2} \right\rangle \left\langle \frac{\tau}{1 + (\omega_c \tau)^2} \right\rangle^{-1} \langle \tau \rangle^{-1}, \quad (2b)$$

where $\omega_c = e B_z / m^*$ is the cyclotron frequency. The coefficient b_M relates to magnetoresistivity, and decreases monotonically with increasing magnetic field. In the limit of a weak magnetic field, $(\omega_c \tau)^2 \ll 1$, the Hall factor r_H converges to $\langle \tau^2 \rangle / \langle \tau \rangle^2$, the value of which lies between 1 and 2 and does not depend on magnetic field. For convenience, the Hall mobility μ_H is defined as $\mu_H = r_H \mu$.

As seen from Eq. (1), the conductivity tensor has the form of a rotational matrix, defining the Hall angle $\theta_H = \arctan(\mu_H B_z)$, by which the current density vector \mathbf{j} deflects from the electric field vector \mathcal{E} in the presence of a normal magnetic field. This fact is commonly used in the classical Hall effect arrangement, where the investigated material is cut into a bar-shaped sample with contacts at the short edges. The characteristic feature of this sample geometry is the vanishing transverse component of the current density even if a magnetic field is applied. Consequently, a transverse field component, the Hall field \mathcal{E}_H , develops, that compensates for the Lorentz force.

The inverse situation occurs in rectangular samples with a great width-to-length ratio, and stripe contacts along the long sides. There the course of the equipotential lines between the contacts is essentially imposed by the parallel contact edges, and the direction of the electric-field vector is thus fixed perpendicular to them. Upon applying a normal magnetic field, the current flow deflects from this direction by the corresponding Hall angle. The resulting elongation of the current path causes an increase of the sample resistance, which is sometimes referred to as the geometrical magnetoresistance.⁸

A question arises about the homogeneity of the electric field in a sample of finite dimensions. There is a generally accepted recommendation for the case of the classical Hall measurement on bar-shaped samples that the length-to-width ratio should be at least 4, in order to eliminate the inhomogeneity of current density distribution near the contacts.^{8,9} From the mathematical point of view the problem of the classical Hall-bar geometry and the problem of the inverse geometry are fully equivalent, as long as the continuity equation combined with Eq. (1) is the adequate description. Its

TABLE I. Sample parameters. The values at 77 K have been obtained by the standard Hall measurement on samples of identical material, and corrected for the presence of depletion layers (Refs. 9 and 14). The values at 1.8 K have been obtained by the presented method and relate to electrons inside the current filaments.

	Sample No. 1	Sample No. 2
Layer thickness	4.3 μm	4.3 μm
Contact distance	1.65 mm	1.65 mm
Contact width	6 mm	6 mm
$n_{77\text{ K}}$	$7.1 \times 10^{15} \text{ cm}^{-3}$	$1.9 \times 10^{15} \text{ cm}^{-3}$
$\mu_{H,77\text{ K}}$	$2.1 \times 10^4 \text{ cm}^2/\text{V s}$	$4.3 \times 10^4 \text{ cm}^2/\text{V s}$
$\mathcal{E}_{h,1.8\text{ K}}$	10.2 V/cm	6.5 V/cm
$n_{1.8\text{ K}}$	$1.3 \times 10^{15} \text{ cm}^{-3}$	$1.5 \times 10^{15} \text{ cm}^{-3}$
$\mu_{H,1.8\text{ K}}$	$1.0 \times 10^4 \text{ cm}^2/\text{V s}$	$3.4 \times 10^4 \text{ cm}^2/\text{V s}$

solution on a rectangular area remains valid, if the vector variables \mathbf{j} and \mathcal{E} are mutually interchanged, along with the corresponding boundary conditions. Therefore, approximately the inverted length-to-width ratio, 1:4, has been chosen in the present experiment.

The rectangular samples were cut from epitaxial layers of *n*-type GaAs grown on a semi-insulating substrate. Two kinds of otherwise identical samples were used, differing in impurity concentration and consequently in electron mobility according to Table I. On each sample a pair of In/Au stripe contacts was alloyed, the distance and width of which were 1.65 and 6 mm, respectively. The sample was immersed in liquid helium inside a superconducting magnet, and illuminated by a set of red light-emitting diodes. The two-dimensional image of the photoluminescence of the sample was recorded by a camera with an infrared sensitive image intensifier.^{4,10} By means of a proper optical filter only the intensity peak corresponding to excitonic recombination was selected, whose intensity is known to drop in the presence of excess free electrons.^{11,12}

Due to the impact ionization of shallow donors, the samples exhibit an electric breakdown, if the sample voltage exceeds a certain threshold voltage. The breakdown field is of a few V/cm, so that intervalley scattering may be disregarded. The typical enhancement in the conductivity during the breakdown is several orders of magnitude, mainly due to the multiplication of the number of free electrons by impact ionization of shallow donors, and partially due to an increase in their mobility. The enhanced conductivity is restricted solely to one or more distinct current filaments, which are formed on account of the system nonlinearity.¹ Though the exact position of the filaments is influenced by sample and contact imperfections, they reveal some elementary generic features: (i) they have well-defined borders which tend to be parallel, forming a stripe-shaped filament with constant critical electric field strength and conductivity inside,² and (ii) their total width is proportional to the total sample current.^{2,10}

Property (i) implies that the Hall angles visualized through the filament tilting relate solely to a single value of the electric field strength inside the current filaments. From the theoretical point of view this critical field strength \mathcal{E}_c corresponds to the coexistence field, which can be deduced

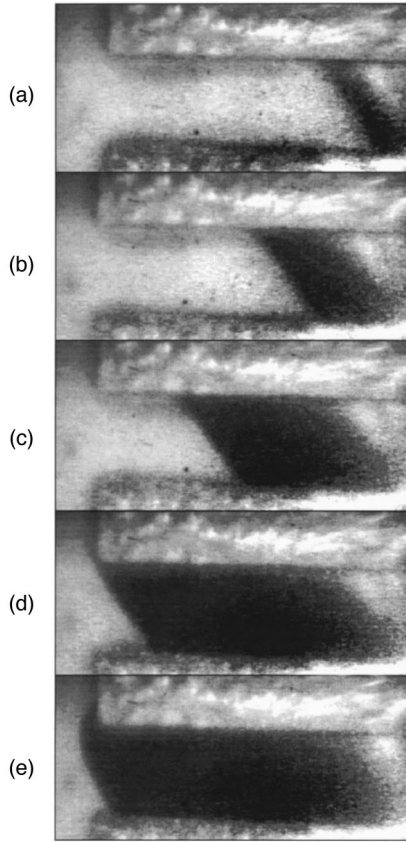
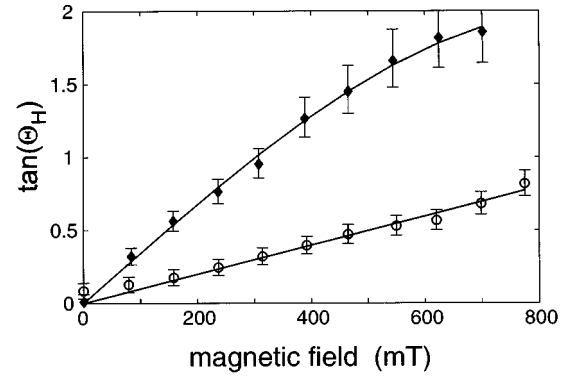


FIG. 2. Visualization of the filamentary current flow at a constant magnetic field $B_z = 309$ mT and (a) $I = 1.17$ mA, (b) $I = 2.32$ mA, (c) $I = 3.82$ mA, (d) $I = 5.99$ mA, and (e) $I = 8.24$ mA.

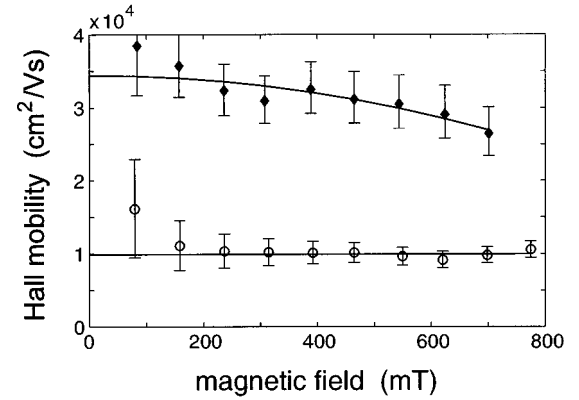
in the framework of the nonequilibrium phase transition theory.¹ The value of \mathcal{E}_c can be determined from the switch-off voltage of the sample, and is indicated for the samples investigated in Table I.

Upon making use of property (ii), one can examine the homogeneity of the field distribution in the sample. In Fig. 2 a series of images at constant magnetic field and varying sample current is shown. While in this case the right filament border remains pinned at a contact imperfection, the left border shifts along the contacts according to the current bias. It can be seen that its slope is preserved except for the vicinity of the contact ends, where the inhomogeneous electric field results in a more complex shape of the filament boundary.

The dependence of the measured Hall angles θ_H on the magnetic-field strength is shown in Fig. 3(a) for the two investigated samples. To reduce the errors due to the pinning of the filament edges on material and contact imperfections, the angle measurements were carried out on several different filament configurations, and averaged. The corresponding Hall mobilities μ_H are plotted in Fig. 3(b). The solid lines represent fitted polynomials of the form $\tan(\theta_H) = \mu_{H0} B_z (1 + k B_z^2)$, reflecting the first-order approximation of Eqs. (1) and (2b). Whereas the Hall mobility in sample No. 1 remains almost constant in a great interval of the magnetic field, in the high-mobility sample (No. 2) μ_H decreases apparently with increasing B_z . This may be attributed to a decrease of the Hall factor r_H , which is expected to vary according to Eq. (2b) with increasing B_z , if the weak-field limit is no longer valid.



(a)



(b)

FIG. 3. (a) Hall angle θ_H and (b) Hall mobility μ_H . Circles and full diamonds depict sample Nos. 1 and 2, respectively. Solid lines are fitted functions of B_z (see text). The error bars correspond to a constant $\pm 3^\circ$ deviation of the angular measurement.

Arguments have been given that in comparable n -type GaAs samples at moderate magnetic fields, the Hall factor r_H lies very close to unity, fluctuating only by about 10% in a wide range of temperatures.⁹ The same result can be found theoretically upon analyzing expression (2b), if the ionized impurity scattering time according to the Brooks-Herring formula^{6,7,9} and the shifted Maxwellian distribution of electron velocities are taken into account. However, the validity of the Brooks-Herring expression is questionable at low temperatures, and, moreover, significant changes of the electron distribution function in the filamentary regime probably occur, as has been shown recently by Monte Carlo simulations.¹³ This may explain the observed decrease of the Hall factor r_H with the magnetic field in case of sample No. 2.

We emphasize that in spite of a possible change of the Hall factor, the description of the galvanomagnetic transport through Eq. (1) remains correct in the whole investigated range of magnetic-field strengths. This is demonstrated by the qualitatively unperturbed character of the current flow, which preserves the form of stripe-shaped current filaments with tilted but straight boundaries.

An estimation of the electron density inside of the current filaments can be obtained, based on the optical measurement of the filament widths. However, possible sources of a significant estimation error must be allowed for. These are, in our case, a potential drop on the contacts and the presence of depletion layers near the surface and the substrate

interface.^{9,14} Whereas the former problem could in principle be avoided by an additional pair of potential-sensing electrodes, the latter one represents a serious difficulty: the estimation of the depletion layer thickness based on the standard theory^{9,14} is questionable due to the uncertainty in the electron distribution function.¹³ Therefore, only the lower limit of the electron density can be calculated in our case, yielding minimum impurity ionization degrees of 0.18 and 0.79 for sample Nos. 1 and 2, respectively.

In conclusion, we have demonstrated that the visualization of the galvanomagnetic transport in a semiconductor sample of proper geometry yields a direct way for measuring

the Hall angle. Additionally, upon analyzing the data obtained on *n*-type GaAs, we have obtained the mobility inside current filaments in the low-temperature breakdown regime, where to our knowledge reliable data have not been available so far. In this regime classical Hall-effect measurements are inapplicable due to the inherent inhomogeneity of current flow and the uncontrollable influence of metallic potential probes on self-organized current filaments.

The authors are indebted to E. Schöll, H. Kostial, and H. Frank for helpful discussions. Financial support by the Deutsche Forschungsgemeinschaft and by the Academy of Sciences of the Czech Republic is gratefully acknowledged.

*Present address: Siemens AG, 81730 München, Germany.

¹E. Schöll, *Nonequilibrium Phase Transitions in Semiconductors* (Springer, New York, 1987).

²V. Novák, J. Hirschinger, W. Prettl, and F.-J. Niedernostheide, *Semicond. Sci. Technol.* **13**, 756 (1998).

³W. Eberle, J. Hirschinger, U. Margull, W. Prettl, V. Novák, and H. Kostial, *Appl. Phys. Lett.* **68**, 3329 (1996).

⁴J. Hirschinger, W. Eberle, W. Prettl, F.-J. Niedernostheide, and H. Kostial, *Phys. Lett. A* **236**, 249 (1997).

⁵A. C. Beer, *Galvanomagnetic Effects in Semiconductors* (Academic, New York, 1963).

⁶K. Seeger, *Semiconductor Physics*, 6th ed. (Springer, Berlin, 1997).

⁷P. Y. Yu and M. Cardona, *Fundamentals of Semiconductors* (Springer, Berlin, 1996).

⁸R. S. Allgaier, *Semicond. Sci. Technol.* **3**, 306 (1988).

⁹G. E. Stillman, in *Handbook on Semiconductors*, edited by T. S. Moss and S. Mahajan (Elsevier, Amsterdam, 1994).

¹⁰J. Hirschinger, F.-J. Niedernostheide, W. Prettl, V. Novák, and H. Kostial, *Phys. Status Solidi B* **204**, 477 (1997).

¹¹O. A. Ryabushkin and V. A. Bader (unpublished).

¹²F. Karel, J. Oswald, J. Pastrňák, and O. Petříček, *Semicond. Sci. Technol.* **7**, 203 (1992).

¹³H. Kostial, M. Asche, R. Hey, K. Ploog, B. Kehrer, W. Quade, and E. Schöll, *Semicond. Sci. Technol.* **10**, 775 (1995).

¹⁴E. H. C. Parker, *The Technology and Physics of Molecular Beam Epitaxy* (Plenum, New York, 1985).